

Selected Paper

Characterization of Non-Native Heme Coordination Structures Emerging upon Guanidine Hydrochloric Acid-Induced Unfolding of *Pseudomonas aeruginosa* Ferricytochrome c_{551}

Hulin Tai, Shigenori Nagatomo, Hajime Mita, Yoshihiro Sambongi,[1] and Yasuhiko Yamamoto*

Department of Chemistry, University of Tsukuba, Tsukuba 305-8571

[1]Graduate School of Biosphere Science, Hiroshima University, Higashi-Hiroshima 739-8528

Received March 30, 2005; E-mail: yamamoto@chem.tsukuba.ac.jp

The non-native heme coordination structures emerging upon guanidine hydrochloric acid (GdnHCl)-induced unfolding of *Pseudomonas aeruginosa* ferricytochrome c_{551} were characterized by absorption, circular dichroism, paramagnetic NMR, and resonance Raman spectroscopy. Hexacoordinated high-spin ferriheme bearing axial His and H_2O ligands, and pentacoordinated high-spin ferriheme with an axial His ligand were identified in the presence of GdnHCl concentrations $\geq$ 1.5 M (M = mol dm^{-3}). These non-native species were rapidly interconverted to each other through cleavage/formation of the Fe–H_2O coordination bond, and were also in dynamic equilibrium, at a rate of $< 2 \times 10^4$ s^{-1}, with the native species. Thus, the present study demonstrated the presence of dynamic equilibrium through cleavage/formation of a Fe–H_2O coordination bond in an unfolding intermediate. These results provide a deeper insight into structure transitions of the heme active site upon folding and unfolding of cytochrome *c*.

The class I cytochromes *c* (cyts *c*) are some among the best-characterized redox-active proteins containing a single heme.[1,2] His and Met residues are coordinated to heme Fe as axial ligands in the native form. However, several different heme coordination structures have been reported, depending on the temperature, pH, ionic strength, and presence of a chemical denaturant or surfactant.[3–12] These non-native heme coordination structures of cyt *c* have attracted the interest of protein researchers because this protein has been recognized as a convenient model for protein folding studies,[6,13] and moreover specific conformational transitions of cyt *c* have been reported to be highly relevant to the biological functions of the protein.[14,15] For example, conformational changes have been thought to be induced in the heme active site of cyt *c* upon complexation with cytochrome *c* oxidase.[14] Furthermore, cyt *c* has been shown to undergo a conformational change early in the reaction cascades of apoptosis.[15] Therefore, we should investigate the structural and physicochemical characteristics of cyt *c* in its non-native form together with the native one in order to fully understand the folding mechanism and the biological functions of the protein.

In the cyt *c* protein scaffold, particularly in the case of oxidized cyt *c* (ferricyt *c*), Fe-bound Met has been shown to be more susceptible to a displacement under non-native conditions, compared with Fe-bound His. Cleavage of the native Fe–Met bond in ferricyt *c* has been shown to occur through local structure changes under various non-native conditions.[3–12] Depending upon the conditions, the Fe–Met bond cleavage in ferricyt *c* results in either a hexacoordinated ferriheme or a pentacoordinated one. A bis-His ferriheme bearing the side-chain of a His residue, other than the axial His as a ligand to heme Fe in place of axial Met, is often formed, and has been shown to act as a kinetic trap for cyt *c* protein folding, which significantly affects the folding mechanism.[16–21] On the other hand, the formation of the pentacoordinated ferriheme of horse and yeast cyts *c* in the presence of a high concentration of micelles of sodium dodecyl sulfate has been characterized in some detail by paramagnetic NMR, and has been discussed in terms of physiological roles of the protein.[8,9]

Cytochrome c_{551} (cyt c_{551}) from *Pseudomonas aeruginosa* is a class I cyt *c*, and is composed of 82 amino acid residues and possesses a single His residue as an axial ligand to heme Fe.[22] Consequently, both unfolding and refolding of this cyt c_{551} proceeds in the absence of the non-native bis-His heme. In the present study, we investigated the non-native heme coordination structures emerging upon guanidine hydrochloric acid (GdnHCl)-induced unfolding of the oxidized cyt c_{551} (ferricyt c_{551}) by absorption, circular dichroism (CD), paramagnetic NMR, and resonance Raman (RR) spectroscopy. An acidic condition, pH 5.00, was used throughout the measurements because of an excellent reversibility of the protein unfolding/refolding process.[23] We found that hexacoordinated high-spin ferriheme bearing axial His and H_2O ligands (6cHS), and pentacoordinated high-spin ferriheme with an axial His ligand (5cHS) prevail in the presence of a high GdnHCl concentration ([GdnHCl]), and that these non-native heme species are rapidly interconverted to each other through cleavage/formation of the Fe–H_2O coordination bond. Furthermore, the 6cHS and 5cHS species were also found to be in dynamic equilibrium, at a rate of $< 2 \times 10^4$ s^{-1}, with the native one, demonstrating that the formation/cleavage of the Fe–Met bond is the rate determining step for interconversion between the native and non-native forms. The present results provide a novel and dynamic description of structure transitions of the heme active site upon GdnHCl-induced unfolding of ferricyt c_{551} in aqueous solution.

Published on the web October 31, 2005; DOI 10.1246/bcsj.78.2019

Experimental

Materials. Cyt c_{551} was produced using *Escherichia coli* and purified as reported previously.[24] Ferricyt c_{551} was prepared by the addition of a 10-fold molar excess of potassium hexacyanoferrate(III). For NMR samples, the protein was concentrated to about 1 mM in an ultrafiltration cell (YM-5, Amicon), and then 100% ^2H_2O was added to the protein solutions. The pH of the sample was adjusted using 0.2 M KOH or 0.2 M HCl and the pH was monitored with a Horiba F-22 pH meter with a Horiba type 6069-10C electrode.

UV–Vis Absorption and CD Measurements. The absorption spectra were recorded at 25 °C with a Beckman DU 640 spectrophotometer and protein concentrations of 0.008 mM and 0.2 mM in 20 mM phosphate buffer, pH 5.00,[25] in the presence of a 10-fold molar excess of potassium hexacyanoferrate(III), were used to measure the heme Soret absorption and 625/695-nm absorption, respectively. The CD spectra were recorded at 25 °C with a JASCO J-720W spectrometer using a protein concentration of 0.005 mM in the identical solution conditions used for the absorption measurements. For a [GdnHCl]-dependence study of the absorption and CD spectra, the protein was incubated in a solution mixture containing various [GdnHCl] at 25 °C for at least 2 h before measurements in order to allow the protein solution to reach equilibration.

The midpoint of the GdnHCl denaturation of the protein was obtained by a linear extrapolation method using the following equation:[26]

$$\theta = \{(\theta_n + m_n[\mathrm{GdnHCl}]) + (\theta_{non} + m_{non}[\mathrm{GdnHCl}]) \times e^{-(\Delta G + g[\mathrm{GdnHCl}])/RT}\}/\{1 + e^{-(\Delta G + g[\mathrm{GdnHCl}])/RT}\}, \quad (1)$$

where θ is the observed molar ellipticity (absorption) and θ_i and m_i (i = n or non for the native and non-native form, respectively) are the intercept and slope of a line drawn for the native or non-native form with the assumption of a linear relationship between θ and [GdnHCl]. ΔG is the free energy change for the conversion of native to non-native protein in the absence of GdnHCl; g is a constant that accounts for the [GdnHCl] dependence of ΔG; R and T represent the gas constant (8.314 $J\,K^{-1}\,mol^{-1}$) and the absolute temperature. Plots of the θ value against [GdnHCl] were fitted using the equation with optimized θ_n, θ_{non}, m_n, m_{non}, ΔG, and g values, as illustrated in Figs. 1 and 3. Then, the midpoint of the GdnHCl denaturation of the protein was calculated from the fitted equation.

^{1}H NMR Measurement. NMR spectra were recorded on a Bruker AVANCE-600 FT NMR spectrometer operating at a ^{1}H frequency of 600 MHz. GdnHCl-d_6 (Cambridge Isotopes) was used as received. Chemical shifts were given in ppm downfield from sodium 4,4-dimethyl-4-silapentane-1-sulfonate with H_2O as an internal reference. Saturation transfer (ST) experiments were carried out by selectively saturating a desired peak for 40 ms, and the resulting spectra were presented in the form of a difference spectrum.

Resonance Raman Measurement. Resonance Raman (RR) spectra were recorded by a liquid nitrogen-cooled charge-coupled device detector (Model LN/CCD-1340-PB, Princeton Instruments) attached to a 75-cm single polychromator (Model 750M, Jobin-Ybon) using excitation with the 413.1 nm line of a Kr laser (Model 2060, Spectra Physics). The slit width and slit height were set to be 150 μm and 20 mm, respectively. The spectral slit width was 7.5 cm^{-1}. The wavenumber width per one channel (resolution) of the detector was 0.5 cm^{-1}. The laser power at the sample point was 1.7 mW. Raman shifts were calibrated with indene, and accuracy of the peak positions of the Raman bands was ±1 cm^{-1}.

Results and Discussion

[GdnHCl] Dependence of the Heme Environment of the Ferricyt c_{551}. We first studied the [GdnHCl] dependence of the heme environment of the ferricyt c_{551} using absorption spectra. In the present study, all of the measurements were car-

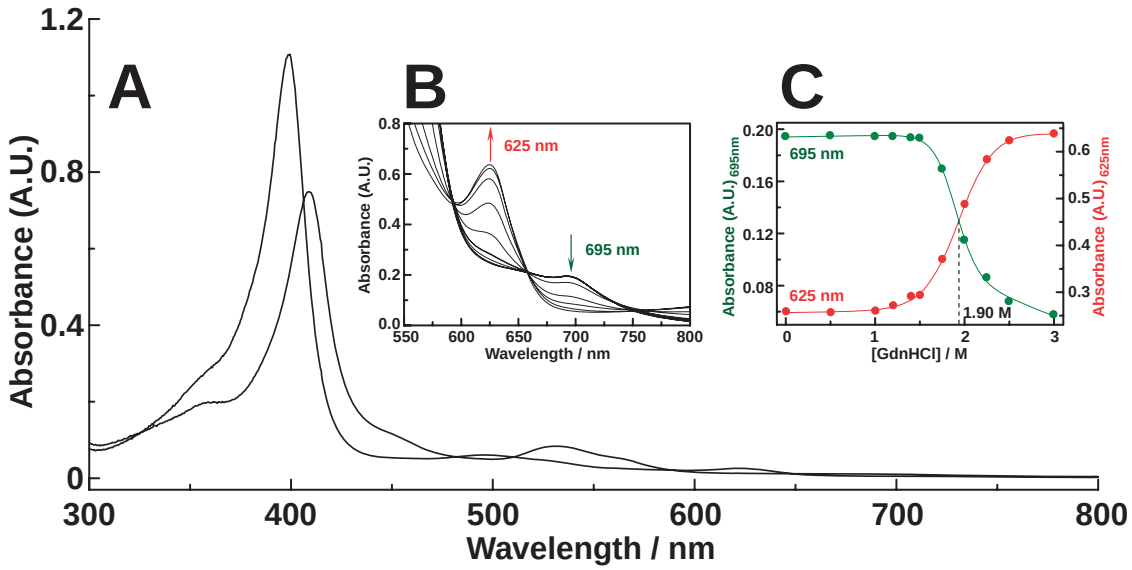

Fig. 1. Absorption spectra, 300–800 nm, of ferricyt c_{551}, pH 5.00, in the absence (λ_{max}: 409, 531.5, and 695 nm) and presence (λ_{max}: 399.5, 495, and 625 nm) of [GdnHCl] = 3 M (M = mol dm^{-3}) at 25 °C (A). Absorption spectra, 550–800 nm, of ferricyt c_{551}, pH 5.00, in the presence of various [GdnHCl] (0–3 M) (B). Isosbestic points were observed at 592, 658, and 752 nm. Plots of 625-nm (red circles) and 695-nm (green circles) absorbance as a function of [GdnHCl] (C). 1.90 ± 0.05 M was obtained as the [GdnHCl] at the transition midpoint (C_m) from both plots.

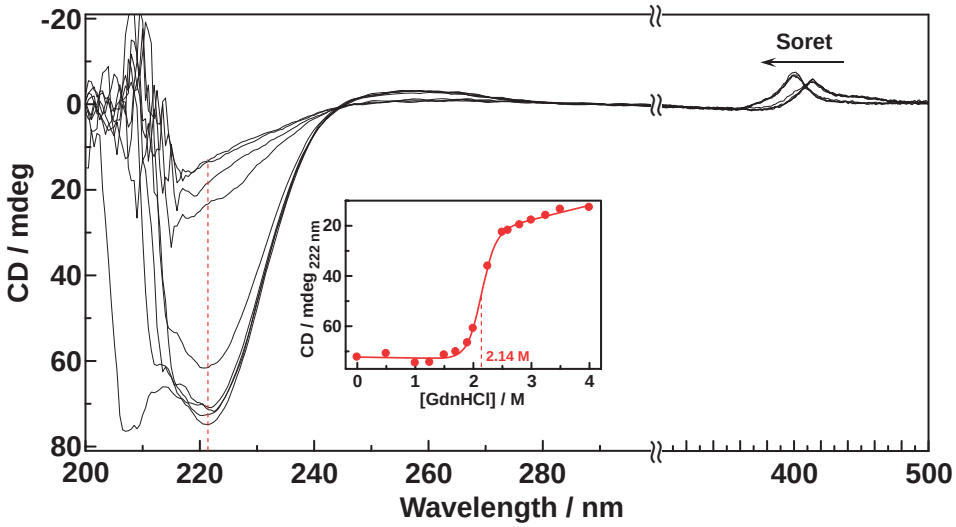

Fig. 2. CD spectra, 200–250 and 350–500 nm, of ferricyt c_{551}, pH 5.00, in the presence of various [GdnHCl] (0–4 M) at 25 °C. Plots of the ellipticity at 222 nm as a function of [GdnHCl] are shown in the inset. 2.14 ± 0.05 M was obtained as the C_m value from the plots.

ried out at pH 5.00, because of an excellent reversibility in the protein unfolding/refolding under an acidic condition, which may be related to the fact that the isoelectric point of the protein is ~4.7.[23] Heme Soret absorption of the native protein at 409 nm exhibited a blue shift to 399.5 nm in the presence of [GdnHCl] = 3 M. The wavelength of heme Soret absorption was shown to be sensitive to the spin and coordination states of heme Fe; the observed wavelength for the unfolded protein, i.e., 399.5 nm, was between the reported values for 6cHS, i.e., ~408 nm, and 5cHS, i.e., ~395 nm, in metmyoglobins (metMbs).[27] Furthermore, with increasing [GdnHCl], 625-nm absorption, attributable to a high-spin (HS) ferriheme complex,[5] emerged and increased in intensity, while the 695-nm absorption characteristic of the Fe–Met bond in the oxidized protein[28,29] decreased, and eventually disappeared (Fig. 1B). Plots of the absorbance at 625 and 695 nm against [GdnHCl] in Fig. 1C demonstrate that the cleavage of the Fe–Met bond occurs concomitantly with the formation of a non-native HS species, giving rise to the 625-nm absorption. Furthermore, the observation of isosbestic points at 592, 658, and 752 nm demonstrated equilibrium between the native and non-native HS species. Fitting the plots in Fig. 1C to a two-state unfolding model, determined by the linear extrapolation method,[26] yielded a [GdnHCl] at the transition midpoint (C_m) of 1.90 ± 0.05 M. The C_m value for the ferricyt c_{551} is almost the same as that of horse ferricyt *c*, judging from the replacement of the Fe-bound Met by a Lys.[21,30]

Characterization of the GdnHCl-Induced Unfolding of the Ferricyt c_{551}. We next characterized the GdnHCl-induced unfolding of the ferricyt c_{551} using CD. Plots of the ellipticity at 222 nm as a function of [GdnHCl] revealed clear two-state unfolding with a C_m value of 2.14 ± 0.05 M (Fig. 2). These results were identical to those previously reported.[3,24] The GdnHCl-induced unfolding curve obtained from the 222-nm ellipticity was compared with that obtained from the 695-nm absorption in Fig. 3. As shown in Fig. 3, the C_m value obtained for the Fe–Met bond cleavage is distinctly lower than that for the overall protein unfolding. This

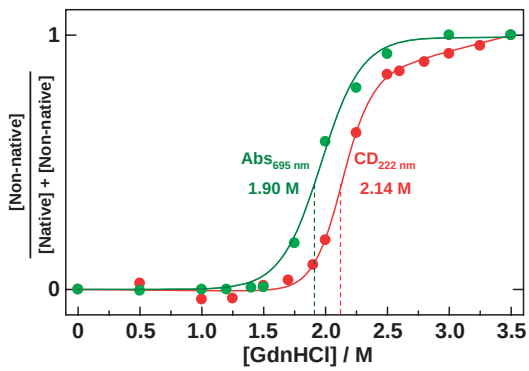

Fig. 3. GdnHCl-induced unfolding curves of ferricyt c_{551}, pH 5.00, at 25 °C, determined on the basis of the 695-nm absorption (green circles) and the 222-nm ellipticity (red circles). The C_m value obtained from the plot of the 695-nm absorption was lower than that from the plot of the 222-nm ellipticity.

finding demonstrated that the Fe–Met bond cleavage precedes the overall protein unfolding during the GdnHCl-unfolding of the ferricyt c_{551}. Consequently, a strengthening of the Fe–Met bond in the ferricyt c_{551} by changing amino acid side chain packing in a hydrophobic core of the protein could enhance the stability of the overall protein structure, as has been demonstrated in a close relationship between the stabilities of the Fe–Met bond and the overall protein structure for homologous proteins.[31]

Characterization of Non-Native Forms Emerging upon the GdnHCl-Induced Unfolding of the Ferricyt c_{551}. We also characterized the heme coordination structure of the non-native HS ferriheme species by paramagnetic NMR. As shown in the 600 MHz ^{1}H NMR spectra (Fig. 4), a new set of signals emerged in the shift range of 55–80 ppm at [GdnHCl] ≥ 1.5 M, and their intensities increased with increasing [GdnHCl]. The characteristics of the GdnHCl-induced unfolding of the present protein under an acidic condi-

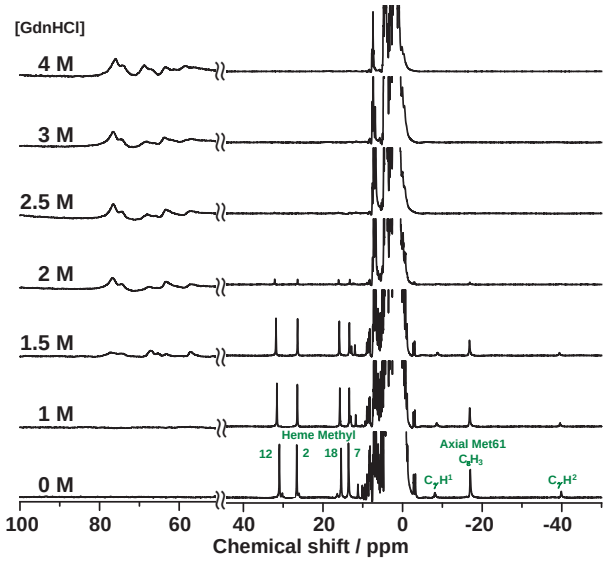

Fig. 4. 600 MHz ^{1}H NMR spectra of ferricyt c_{551}, p^{2}H 5.00, in the presence of various [GdnHCl] (0–4 M) at 25 °C. The assignments of heme methyl and axial Met proton signals were indicated in the spectra. A new set of signals emerged in the shift range of 55–80 ppm at [GdnHCl] = 1.5 M, and their intensities increased with further increasing [GdnHCl].

tion are manifested in the spectral changes shown in Fig. 4. First, only signals due to native protein were resolved in the chemical shift range of 15–35 ppm, where signals due to low-spin (LS) ferriheme appear. This is quite different from the results of similar GdnHCl-induced unfolding studies of other ferricyts *c*, which generally reflected the presence of multiple non-native LS forms, such as bis-His and His–Lys ferrihemes. Due to a lack of His residues other than axial His in the protein, the formation of bis-His ferriheme can be ruled out. Furthermore, the unfolding of ferricyt *c* under an acidic condition hampers the coordination of the side-chain of a Lys to heme Fe in a non-native protein, through the ionization of its side chain; in fact, signals attributable to His–Lys ferriheme were identified in the spectra of non-native forms, which emerge upon the GdnHCl-induced unfolding of the protein under a physiological pH condition (results not shown). Second, the [GdnHCl]-dependent spectral changes of the protein are completely reversible, as has been demonstrated previously.[23] The shifts of the newly emerging signals were the same as those of the heme methyl proton signals of a typical HS ferriheme species.[32] The newly emerging methyl proton signals were identified and assigned by saturation transfer (ST) experiments (Fig. 5). Saturation of the heme methyl proton signals of non-native HS ferriheme yielded the ST connectivities to the assigned heme methyl proton signals of native ferricyt c_{551},[33] which facilitated unambiguous assignments for the non-native signals. The heme methyl proton shift pattern of 7-, 12-, 18-, and 2-methyl signals, in the order of decreasing the shift, for the non-native HS ferriheme is similar to that obtained for non-native HS form emerged upon the GdnHCl-induced unfolding of *Bacillus pasteurii* ferricyt *c*, although the shifts are larger by more than 7 ppm in the former than the latter.[6] On the other hand, the mean heme methyl proton shift of 72.7 ppm for the non-native HS ferriheme at 25 °C was almost the same as the value for sperm whale metMb, in which both axial His and H_2O are coordinated to Fe^{3+} of a *b*-type heme.

The heme methyl and axial Met proton signals of the ferricyt c_{551} were resolved from the diamagnetic envelope where protein proton signals severely overlap,[33] and their intensities decreased with increasing [GdnHCl], and vanished at [GdnHCl] = 3 M, although their shifts were only slightly affected by GdnHCl. On the other hand, the line widths of the native signals were greatly increased in the presence of [GdnHCl] > 2 M. The [GdnHCl]-dependent behavior of the NMR signal intensities for the native and newly emerging species paralleled, within experimental errors, that of the Fe–Met bond cleavage, as determined by an analysis of the 695-nm absorption, and the HS ferriheme species giving rise to the 625-nm absorption, respectively. These results strongly suggested that the HS species detected in the absorption and NMR spectra were identical with each other. Since the signals for both the native and non-native HS species were separately observed in the NMR spectra, the time scale of the interconversion between them was found to be slower than the NMR time scale, and a value of 2×10^4 s^{-1} was estimated to be the upper limit of the interconversion rate from the difference in the resonance frequency between the signals of the two species. These results indicated that the formation/cleavage of Fe–Met bond is the rate determining step for the interconversion between the native and non-native forms of the protein.

Characterization of Heme Coordination Structure of Non-Native High-Spin Ferriheme of the Ferricyt c_{551}. Characterization of the heme coordination structure of the non-native HS ferriheme was carried out through an analysis of the influence of the solvent isotope composition on the shifts and line widths of paramagnetically shifted heme methyl proton NMR signals, as reported previously.[34] La Mar et al.[34] found larger paramagnetic shifts and line widths of heme methyl proton signals for 6cHS species in metMbs and methemoglobins (metHb) in ^2H_2O than ^1H_2O, while such isotope effects were not observed for the 5cHS species. Therefore, the influence of the solvent isotope composition on the shifts and line widths of the heme methyl proton NMR signals could serve as a probe for the presence of a water molecule coordinated to heme Fe. All of the heme methyl proton signals of the HS ferriheme species in ^2H_2O exhibited downfield shifts of 0.5–1.3 ppm relative to the corresponding signals in ^1H_2O, although the line widths were essentially the same (Fig. 6). The observed isotope effects on the signals of the present HS ferriheme species were somewhat smaller than those reported for 6cHS species in metMb or metHb, i.e., ~1.5 ppm.[34] These results could be interpreted in terms of a partial occupancy of an exogenous H_2O ligand in the present HS ferriheme species, as demonstrated for elephant metMb, in which formation/cleavage of the Fe–H_2O bond occurs rapidly.[35] Moreover, the line widths of the signals for the present HS ferriheme species ranged >1300 Hz, and thus were considerably larger than those for the heme methyl proton signals of the typical 6cHS and 5cHS species in hemoproteins possessing comparable molecular weights to cyt c_{551}, i.e., 300–700 Hz.[36] The

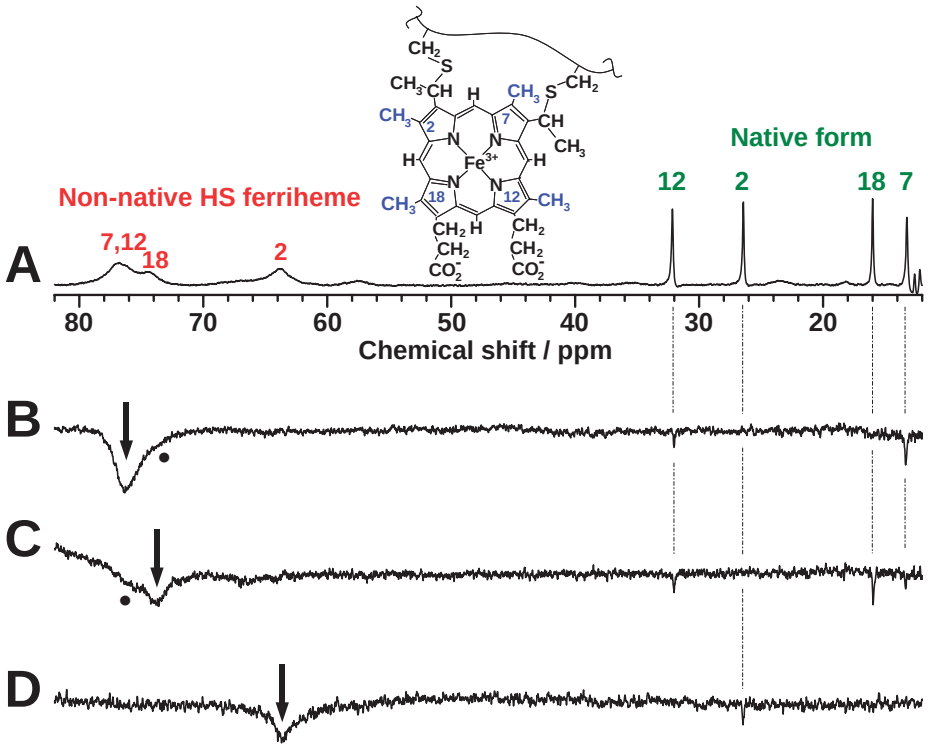

Fig. 5. 600 MHz ^{1}H NMR spectrum and saturation transfer (ST) difference spectra of ferricyt c_{551}, p^{2}H 5.00, in the presence of [GdnHCl] = 2 M at 25 °C. The molecular structure and numbering system of heme is illustrated in the inset. The assignments of the heme methyl proton (2-, 7-, 12-, and 18-Me) signals of non-native HS ferriheme in the shift range of 60–80 ppm were indicated in the spectra. (A) Reference spectrum. (B) ST difference spectrum on resulted from simultaneous saturation of two methyl proton signals at ~77 ppm yielded a ST effect to both 7- and 12-Me signals of native ferricyt c_{551}. (C) ST difference spectrum on saturation of a methyl proton signal at ~74 ppm yielded a ST effect to 18-Me signal of the native protein. Small ST effects observed on 7- and 12-Me signals of the native protein are attributed to a decoupler power spillage, as indicated by a black circle. (D) ST difference spectrum resulted from a methyl proton signal at ~64 ppm yielded a ST effect to 2-Me signal of the native protein. In (B)–(D), peak being saturated is indicated by an arrow.

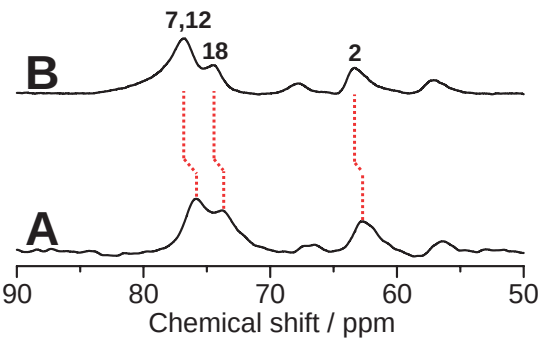

Fig. 6. Downfield-shifted portion of the 600 MHz ^{1}H NMR spectra of ferricyt c_{551}, pH 5.00, in ^1H_2O (A) and ^2H_2O (B) at 25 °C. The signals in trace B exhibited downfield shifts of 0.5–1.3 ppm relative to the corresponding signals in trace A, although the line widths were essentially the same.

considerably larger line widths of the signals for the present HS ferriheme species could be attributed to the dynamic exchange broadening between the 6cHS and 5cHS species, as reported for elephant metMb.[35] Since the pK_a value of Fe-bound His was reported to be ~3,[12,37] the dynamic exchange process between the non-native 6cHS and 5cHS species was not attributed to the formation/cleavage of Fe–His bond, but to that of the Fe–H_2O bond. This finding indicates that the thermodynamic stability of the 6cHS form with an exogenous H_2O ligand is a determinant of the reaction path of the folding/unfolding of the protein as well as its dynamic properties. Although two different species, 6cHS and 5cHS, are present as non-native forms upon the GdnHCl-induced unfolding of the protein at pH 5.00, an apparent two-state unfolding was clearly manifested in observing the isosbestic points in the absorption spectra (Fig. 1). This result indicated that the equilibration of the interconversion between the non-native 6cHS and 5cHS species is independent of [GdnHCl]. This result indicate that the thermodynamic stabilities of the non-native 6cHS and 5cHS forms are not affected by the protein structure, but are related to the stabilities of their coordination structures. In addition, the apparent two-state unfolding observed in the [GdnHCl]-dependent 222-nm ellipticity (Fig. 3) demonstrated that the protein foldings of the non-native 6cHS and 5cHS forms are highly similar.

The formation of both 6cHS and 5cHS species was detected in the RR spectra recorded with excitation at 413.1 nm (Fig. 7). Increasing [GdnHCl] caused a growing-in of the characteristic HS marker bands, i.e., ν_3 and ν_2 at 1485 and 1572 cm^{-1}, re-

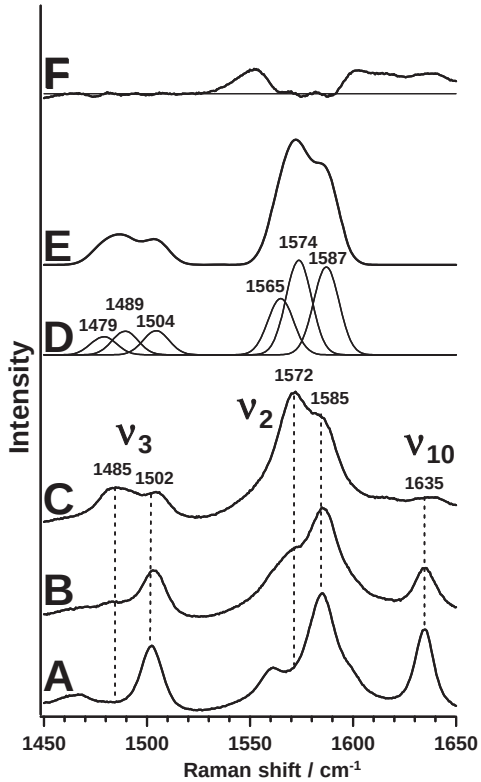

Fig. 7. RR spectra of ferricyt c_{551}, pH 5.00, in the absence (A) and presence of [GdnHCl] = 2 M (B) and 4 M (C). (D) The component peaks and (E) resultant simulated spectrum to fit trace C. 6cHS, 5cHS, and 6cLS were manifested in the ν_3 and ν_2 bands; 6cHS: ν_3 (1479 cm^{-1}) and ν_2 (1565 cm^{-1}), 5cHS: ν_3 (1489 cm^{-1}) and ν_2 (1574 cm^{-1}); and 6cLS: ν_3 (1504 cm^{-1}) and ν_2 (1587 cm^{-1}). (F) Residual as a result of the subtraction of trace C from trace E.

spectively, at the expense of the corresponding LS bands, i.e., ν_3 and ν_2 bands at 1502 and 1585 cm^{-1}, respectively, and also the ν_{10} band at 1635 cm^{-1}. The broad ν_3 and ν_2 bands in Fig. 7C could be simulated with the three bands at 1479, 1489, 1504 cm^{-1} and 1565, 1574, 1587 cm^{-1}, respectively (Figs. 7D and 7E). The ν_3 and ν_2 bands at 1479 and 1565 cm^{-1} could be attributed to 6cHS, and those at 1489 and 1574 cm^{-1} to 5cHS.[38,39] The RR results confirmed the coexistence of the 6cHS and 5cHS forms of ferricyt c_{551} in the presence of high [GdnHCl].

In contrast to the detection of both the non-native 6cHS and 5cHS forms in the present protein, only the 5cHS form was detected as a non-native HS form in horse and yeast ferricyts *c* with a high concentration of micelles of sodium dodecyl sulfate.[8,9] An exogenous water ligand, indispensable for the formation of the 6cHS form, is likely to be excluded from the heme coordination site within the non-polar environment provided by the micelles. Furthermore, Gianni et al.[3] reported that the Fe–Met cleavage form is a high energy native-like intermediate, and that it never accumulates in time-resolved kinetic experiments. The present study, however, clearly demonstrated, from both ^{1}H NMR and RR, the coexistence of the 6cHS and 5cHS forms. The Fe–Met cleavage form, i.e., 5cHS and 6cHS, observed in this study, may possess various contents of the secondary structure, depending upon [GdnHCl], and may be different from the Fe–Met cleavage form detected in the time-resolved kinetic studies in terms of the protein structure. Therefore, the thermodynamic stability of the Fe–Met cleavage form could be different to each other.

Conclusion

The present study demonstrated that rapidly interconverting 5cHS and 6cHS forms emerged as non-native species upon GdnHCl-induced unfolding of ferricyt c_{551} in aqueous solution at pH 5.00, and that both the 5cHS and 6cHS species were in dynamic equilibrium, at a rate of $< 2 \times 10^4$ s^{-1}, with the native one. The rapid interconversion between the non-native 5cHS and 6cHS forms dictated that the formation/cleavage of Fe–H_2O coordination bond was faster than the NMR time scale. Since the conversion of the 6cHS form to the native form or vice versa has to occur through the 5cHS one, the relatively slow interconversion between the native and non-native forms of the protein indicated that the formation/cleavage of the Fe–Met bond is the rate determining step for the processes. The roles of the 6cHS form concerning the thermodynamic and dynamic properties, and the energy landscape of the protein folding remain to be elucidated.

We wish to thank Professor Teizo Kitagawa, National Institutes of Natural Sciences, for the use of the resonance Raman equipment. The ^{1}H NMR spectra were recorded on a Bruker AVANCE-600 spectrometer at the Chemical Analysis Center, University of Tsukuba. This work was supported by a research grant (No. 17530081) from the Ministry of Education, Culture, Sports, Science and Technology of Japan.

References

1 G. R. Moore and G. W. Pettigrew, "Cytochromes *c*: Evolutionary, Structural, and Physicochemical Aspects," Springer-Verlag, Berlin (1990).

2 R. A. Scott and A. G. Mauk, "Cytochrome *c*: A Multidisciplinary Approach," Univ. Science Books, Sausalito (1996).

3 S. Gianni, C. Travaglini-Allocatelli, F. Cutruzzolà, M. G. Bigotti, and M. Brunori, *J. Mol. Biol.*, **309**, 1177 (2001).

4 F. Cutruzzolà, M. Arese, G. Ranghino, G. Van Pouderoyen, G. Canters, and M. Brunori, *J. Inorg. Biochem.*, **88**, 353 (2002).

5 S. Oellerich, H. Wackerbarth, and P. Hilderbrandt, *J. Phys. Chem. B*, **106**, 6566 (2002).

6 I. Bartalesi, I. Bertini, K. Ghosh, A. Rosato, and P. Turano, *J. Mol. Biol.*, **321**, 693 (2002).

7 M. Assfaig, I. Bertini, A. Dolfi, P. Turano, A. G. Mauk, F. I. Rosell, and H. B. Gray, *J. Am. Chem. Soc.*, **125**, 2913 (2003).

8 S. Chevance, E. Le Rumeur, J. D. De Certaines, G. Simonneaux, and A. Bondon, *Biochemistry*, **42**, 15342 (2003).

9 I. Bertini, P. Turano, P. R. Vasos, A. Bondon, S. Chevance, and G. Simonneaux, *J. Mol. Biol.*, **336**, 489 (2004).

10 S. J. Berners-Price, I. Bertini, H. G. Gray, G. A. Spyroulias, and P. Turano, *J. Inorg. Biochem.*, **98**, 814 (2004).

11 B. S. Russell, R. Melenkivitz, and K. L. Bren, *Proc. Natl. Acad. Sci. U.S.A.*, **97**, 8312 (2000).

12 S.-R. Yeh, S. W. Han, and D. L. Rousseau, *Acc. Chem. Res.*, **31**, 727 (1998).

13 M. Brunori, M. G. Bigotti, F. Cutruzzolà, S. Gianni, and C. Travaglini-Allocatelli, *Biophys. Chem.*, **100**, 409 (2003).

14 S. Döpner, P. Hildebrandt, F. I. Rosell, A. G. Mauk, M. von Walter, G. Buse, and T. Soulimane, *Eur. J. Biochem.*, **261**, 379 (1999).

15 R. Jemmerson, J. Liu, D. Hausauer, K. P. Lam, A. Mondino, and R. D. Nelson, *Biochemistry*, **38**, 3599 (1999).

16 G. A. Elöve, A. K. Bhuyan, and H. Roder, *Biochemistry*, **33**, 6925 (1994).

17 S.-R. Yeh, S. Takahashi, B. Fan, and D. L. Rousseau, *Nat. Struct. Biol.*, **4**, 51 (1997).

18 J. R. Telford, F. A. Tezcan, H. B. Gray, and J. R. Winkler, *Biochemistry*, **38**, 1944 (1999).

19 A. Arcovito, S. Gianni, M. Brunori, C. Travaglini-Allocatelli, and A. Bellelli, *J. Biol. Chem.*, **276**, 41073 (2001).

20 T. R. Sosnick, L. Mayne, R. Hiller, and S. W. Englander, *Nat. Struct. Biol.*, **1**, 149 (1994).

21 W. Colon, L. P. Wakem, F. Sherman, and H. Roder, *Biochemistry*, **36**, 12535 (1997).

22 Y. Matsuura, T. Takano, and R. E. Dickerson, *J. Mol. Biol.*, **156**, 389 (1982).

23 J. Hasegawa, Doctoral Thesis, The University of Tokyo (2002).

24 J. Hasegawa, H. Shimahara, M. Mizutani, S. Uchiyama, H. Arai, M. Ishii, K. Kobayashi, S. J. Ferguson, Y. Sambongi, and Y. Igarashi, *J. Biol. Chem.*, **274**, 37533 (1999).

25 The pH meter reading has been shown to underestimate the pH value of bulk solution in the presence of high salt concentration (M. M. Garcia-Mira and J.-M. Sanchez-Ruiz, *Biophys. J.*, **81**, 3489 (2001)). At [GdnHCl] = 4 M, which is the highest concentration used in the study, the pH value differs from the pH meter reading by as much as −0.4. On the other hand, as far as the effect of pH on cyt c_{551} structure is concerned, the pH meter reading may represent the net concentration of hydrogen ion which interacts with the protein. Therefore, we adopted the pH meter reading to represent the pH value, irrespective of [GdnHCl], throughout the manuscript. In addition, the results presented in the manuscript are not so sensitive to pH that the pH correction has no significant influence on the data interpretation.

26 M. M. Santaro and D. W. Bolen, *Biochemistry*, **27**, 8063 (1988).

27 K. Shikama and A. Matsuoka, *J. Mol. Biol.*, **209**, 489 (1989).

28 A. Schejter and P. George, *Biochemistry*, **3**, 1045 (1964).

29 E. Shechter and P. Saludjian, *Biopolymers*, **5**, 788 (1967).

30 B. S. Russell and K. L. Bren, *J. Biol. Inorg. Chem.*, **7**, 909 (2002).

31 Y. Yamamoto, N. Terui, T. Tachiiri, K. Minakawa, H. Matsuo, T. Kameda, J. Hasegawa, Y. Sambongi, S. Uchiyama, Y. Kobayashi, and Y. Igarashi, *J. Am. Chem. Soc.*, **124**, 11574 (2002).

32 I. Bertini and C. Luchinat, "NMR of Paramagnetic Molecules in Biological Systems," Benjamin/Cummings, Menlo Park (1986), pp. 165–229.

33 R. Timkovich and M. Cai, *Biochemistry*, **32**, 11516 (1993).

34 G. N. La Mar, M. J. Chatfield, D. H. Peyton, J. S. De Ropp, W. S. Smith, R. Krishnamoorthi, J. D. Satterlee, and J. E. Erman, *Biochim. Biophys. Acta*, **956**, 267 (1988).

35 R. Krishnamoorthi, G. N. La Mar, H. Mizukami, and A. E. Romero-Herrera, *J. Biol. Chem.*, **259**, 265 (1984).

36 Y. Yamamoto, A. Ōsawa, Y. Inoue, R. Chûjô, and T. Suzuki, *Eur. J. Biochem.*, **192**, 225 (1990).

37 M. G. Bigotti, C. T. Allocatelli, R. A. Staniforth, M. Arese, F. Cutruzzolà, and M. Brunori, *FEBS Lett.*, **425**, 385 (1998).

38 T. Kitagawa, Y. Kyogoku, T. Iizuka, and M. I. Saito, *J. Am. Chem. Soc.*, **98**, 5169 (1976).

39 T. G. Spiro and J. M. Burke, *J. Am. Chem. Soc.*, **98**, 5482 (1976).